Relativistic acceleration in noninertial frames of a line of objects

Chris Dobson[a)]
NASA/MSFC, Huntsville, Alabama 35812

(Received 30 January 2023; accepted 14 December 2023)

A general solution to the problem of relativistic acceleration of point objects in the noninertial frame of any of the objects is given in one spatial dimension. The objects are initially at rest in a common inertial frame and accelerate until they are at rest in a second inertial frame. The starting time and position of each object, the acceleration rate of each object, and the number of objects are arbitrary. The solution gives the position and velocity of each object in the noninertial frame of the host object, and the proper time of each, as functions of the proper time of the host. The method is based on system states for a pair of objects, and it is found that there are nine series of states which cover all cases, including those in which objects are separated from the host by its Rindler horizon. The familiar problems of acceleration of an elastic rod and a (Born) rigid rod are treated, and a number of examples are given of spaceflight sequences for multiple craft in tandem.
https://doi.org/10.1119/5.0144523

NOMENCLATURE

a	Proper acceleration of the ship
b	Proper acceleration of the escort
c	Speed of light in vacuum
$d, d', \hat{d}$	Position coordinates of escort launch in $S, S', \hat{S}$
$f(z)$	The function $\sqrt{1+z^2}$
S	Initial inertial frame; coordinates x, t
S'	Final inertial frame; coordinates x', t', velocity v in S
$\hat{S}(u)$	instantaneous rest frames; coordinates $\hat{x}$, $\hat{t}$, velocities u in S
$\underline{t}$	Dimensionless coordinate time variable
t_{au}	Elapsed coordinate time, velocity u, acceleration a
t_a	Characteristic time scale for acceleration a
x_a	Characteristic distance scale for acceleration a
α_u	Product $\beta_u\gamma_u$
β	Velocity ratio of escort in Σ
β_u	Ratio of velocity u to c
γ_u	Lorentz factor for velocity u
δ, δ'	Time coordinates of escort docking in S, S'
η_j	Horizon parameter, escort in state j at ship launch
$\lambda, \lambda', \hat{\lambda}$	Time coordinates of escort launch in $S, S', \hat{S}$
μ_u	Rapidity for velocity u
ξ	Position coordinate of escort in Σ
v	Velocity of S' in S
ρ	Proper time of the escort
Σ	Rest frame of the ship, successively comoving with $\hat{S}(u)$ for $0 \le u \le v$
τ	Proper time of the ship
$\underline{\tau}$	Dimensionless proper time variable
τ_{au}	Elapsed proper time, velocity u, acceleration a
$\tau_{ij,i'j'}$	Proper time of ship for transition between ψ_{ij} and $\psi_{i'j'}$
ψ_{ij}	State of system with ship state i and escort state j

I. INTRODUCTION

Relativistic acceleration in Minkowski space is important in a variety of kinematic problems and also connects to gravitational dynamics.[1,2] Interesting effects have been noted in the acceleration of extended objects,[3–6] which are modeled as arrays of point objects. Solution in the accelerated frame is often of interest in these kinematic problems, though the treatment is typically piecemeal and *ad hoc*. More broadly, accelerated frames anchor studies in areas as diverse as vacuum and quantum effects.[7–9]

We have organized a systematic solution to the problem of acceleration of point objects in noninertial frames in one spatial dimension. An array of independent objects begins at rest in one inertial frame and accelerates until it comes to rest in a second inertial frame. Each object has its own rate of acceleration and its own starting time and position as input parameters. The solution gives the position and velocity of object m in the rest frame of object m^* and the proper time of object m as functions of the proper time of object m^* for arbitrary objects m and m^* in the array. The object m^* is the host object and m is its companion.

The analysis is based explicitly on states of a two-object system, m and m^*, defined by the acceleration status of each. There are nine series of such states possible, deriving from arrangements of the acceleration periods and from the Rindler horizon of the host object m^*. The applicable series for a given problem, the object motions in each state, and the times of transitions between states are uniquely determined by the input parameters. A sequence index is also introduced, to distinguish among horizon cases within a series.

In what follows, the acceleration problem will be discussed largely in terms of a spaceship, object m^*, and its escort, object m, a concrete and convenient example. The focus, then, is on solution in the rest frame of the ship for a train of accompanying escorts on an extended spaceflight. To be clear, though, the solution applies to problems on any scale, so long as the objects may be considered as points on that scale. Section II gives the equations of motion for constant acceleration, the coordinate frames, and key event coordinates. Section III defines the system states and tabulates equations for each, and Sec. IV analyzes the state series, detailing the effects of the Rindler horizon and defining the flight sequences. Section V then surveys the results, illustrating the solution with a number of examples. This includes the laboratory-scale problems of acceleration of elastic and rigid rods as well as independent spaceflight problems with constraints analogous to Born rigidity.

The solution to the acceleration problem describes the experience of the spaceflight aboard the ship. The acceleration of the ship subjects its occupants to a steady force, but otherwise goes unnoticed within the ship itself. By contrast, the effect of the acceleration on the position, velocity, and time rate of the escorts relative to the ship is striking, and particularly when the escorts too are accelerating. The escort events are typically remote and, thus, not observable in real time on the ship, but in an actual flight they could eventually be reconstructed by shipboard observers.

A summary of the notation used in this paper is given in the Nomenclature. The quantities in the Nomenclature are introduced and defined in Secs. II–IV.

II. EQUATIONS OF MOTION

The host object is represented by a spaceship, and its companion is an escort craft. The solution to the acceleration problem, thus, gives the motion of the escort in the rest frame of the ship, denoted Σ. The spacecraft begin parked on launchpads at rest in the inertial frame S, and at the end of their journey, they dock to a space station at rest in inertial frame S'. The frame S' is in standard configuration[1] with S and its speed with respect to S is v.

For generic velocity u, the Lorentz factor γ, the rapidity μ, and two related terms are defined with velocity subscripts,

$$\beta_u = \frac{u}{c}, \tag{1a}$$

$$\gamma_u = \frac{1}{\sqrt{1-\beta_u^2}}, \tag{1b}$$

$$\alpha_u = \beta_u \gamma_u, \tag{1c}$$

$$\mu_u = \operatorname{artanh} \beta_u = \operatorname{arcosh} \gamma_u = \operatorname{arsinh} \alpha_u, \tag{1d}$$

where the last two equalities follow from the properties of the hyperbolic functions. For generic acceleration a, define

$$t_a = \frac{c}{a}, \tag{2a}$$

$$x_a = c t_a, \tag{2b}$$

$$t_{au} = t_a \alpha_u, \tag{3a}$$

$$\tau_{au} = t_a \mu_u. \tag{3b}$$

Equations (2a) and (2b) give characteristic time and distance scales, and Eqs. (3a) and (3b), derived below, are trip times, durations of coordinate and proper time required of a fixed acceleration to achieve a particular velocity.

The proper acceleration a is in the frame of the accelerated object. Let x and t be the coordinates and $u = dx/dt$ the speed of the object in S, and let τ be the object's proper time. Formally, the proper acceleration is the magnitude of the four-acceleration, which here is $a = \gamma_u^2 (du/d\tau)$.[1,10,11] The equations of motion for an object with proper acceleration a are determined by integration of this equation, and for constant a, they are,[1]

$$u = c \tanh \underline{\tau}, \tag{4a}$$

$$x = x_0 + x_a\left(\cosh \underline{\tau} - \gamma_{u_0}\right), \tag{4b}$$

$$t = t_0 + t_a\left(\sinh \underline{\tau} - \alpha_{u_0}\right), \tag{4c}$$

where we have defined the dimensionless proper time variable,

$$\underline{\tau} = (\tau - \tau_0)/t_a + \mu_{u_0}, \tag{4d}$$

and the subscript "0" denotes initial values, at the lower bounds of the integrals of the acceleration equation. Note that this model has jump discontinuities in the acceleration at its endpoints.[11]

Equations (4a)–(4d) determine the motion and are complete as written. However, the form

$$f(\underline{t}) = \sqrt{1 + \underline{t}^2} \tag{5}$$

is also in common use[3,4] and gives

$$\tanh \underline{\tau} = \underline{t}/f(\underline{t}), \tag{6a}$$

$$\cosh \underline{\tau} = f(\underline{t}), \tag{6b}$$

$$\sinh \underline{\tau} = \underline{t}, \tag{6c}$$

where, from Eq. (4c), the dimensionless coordinate time variable is defined as

$$\underline{t} = (t - t_0)/t_a + \alpha_{u_0}. \tag{6d}$$

Equations (6a)–(6d) can be used, for example, to simplify expressions for $u(t)$ and $x(t)$ from Eqs. (4a)–(4d). They are used in Sec. III to simplify state equations. Equations (4a)–(4d) are given in dimensioned form, and for transparency, the development here retains this form. It is useful, however, to normalize the time and space variables to the scales in Eqs. (2a) and (2b), and this is done in the graphs. Normalization is discussed more fully in Sec. V. Also note that Eqs. (4b) and (4c) correspond, with appropriate choice of constants, to transformation relations for Rindler coordinates x_R, t_R.[12] The Rindler frame comoves with the accelerating object so that the object's position coordinate x_R is a constant and its coordinate time t_R is its proper time. With $t_0 = \tau_0 = u_0 = 0$ and $x_0 = x_a$, Eqs. (4b) and (4c) give $\tau = t_a \operatorname{artanh}(ct/x) = t_R$, and substituting this in either equation gives $x_a = \sqrt{x^2 - (ct)^2} = x_R$.[12] Rindler coordinates are useful for indefinitely sustained accelerations, and the separations of lines of constant x_R correspond to differences in x_0 required to achieve Born rigidity for the respective accelerations (see Sec. IV D).

The equations of motion (4a)–(4d) apply in any inertial frame, and to any object. For the ship, the launch coordinates, for convenience and without loss of generality, are set to $x_0 = t_0 = x'_0 = t'_0 = 0$, where x', t' are the coordinates of S'. For both the ship and the escort, the initial velocity in S is zero, and in S' it is $-v$. The S launch coordinates of the escort are $x_0 = d$ and $t_0 = \lambda$, and in S', these are $x'_0 = d'$ and $t'_0 = \lambda'$, where $d' = \gamma_v d - \alpha_v \lambda c$ and $\lambda' = \gamma_v \lambda - \alpha_v d/c$, from Eqs. (1b) and (1c) with $u = v$. The proper acceleration of the ship is a and that of the escort is b, both positive. The symbol τ without a subscript is used generically in Eqs. (4a)–(4d) and (6a)–(6d) but otherwise denotes the proper time of the ship, zero at $t = 0$, and the proper time of the escort is denoted ρ.

Some useful general information may be obtained immediately from Eqs. (4a)–(4d). The proper time required for the ship to reach velocity u is, from Eqs. (4a), (4d), and (1d), $\tau = t_a \mu_u$, or, from Eq. (3b)

Table I. Event coordinates in the launch and docking frames.

	Ship launch	Escort launch	Ship docking	Escort docking
S	$t=0$	$t=\lambda$	$t=t_{av}$	$t=\delta$
	$x=0$	$x=d$	$x=x_a(\gamma_v-1)$	$x=d+x_b(\gamma_v-1)$
S'	$t'=0$	$t'=\lambda'$	$t'=t_{av}$	$t'=\delta'$
	$x'=0$	$x'=d'$	$x'=x_a(1-\gamma_v)$	$x'=d'+x_b(1-\gamma_v)$

$$\tau(u)=\tau_{au}. \tag{7a}$$

At docking, then, $\tau=\tau_{av}$ is the trip time. For the escort in S, Eq. (4d) is $\underline{\rho}=(\rho-\lambda)/t_b$, so that $\rho=\lambda+t_b\mu_u$, and at docking,

$$\rho=\lambda+\tau_{bv}. \tag{7b}$$

Equation (4c) then gives the duration of the trip in coordinate time and Eq. (4b) the acceleration distance. For the ship, $t=t_a\sinh(\tau_{av}/t_a)$, $x=x_a[\cosh(\tau_{av}/t_a)-1]$, $t'=t_a[\sinh(\tau_{av}/t_a+\mu_{-v})-\alpha_{-v}]$, and $x'=x_a[\cosh(\tau_{av}/t_a+\mu_{-v})-\gamma_{-v}]$. For the escort, the equations are very similar, but include λ and d. It is also useful to explicitly define symbols for the escort docking times,

$$\delta=\lambda+t_{bv}, \tag{8a}$$

$$\delta'=\lambda'+t_{bv}, \tag{8b}$$

where, from Eq. (3a), $t_{bv}=t_b\alpha_v$. These results are summarized in Table I, which lists the launch and docking coordinates in the terminal inertial frames.

A noninertial frame is modeled on a continuous succession of inertial frames.[1] A set of inertial frames $\hat{S}(u)$, each in standard configuration with S and moving with velocity u in S, is defined, one frame for each ship velocity u; the coordinates are $\hat{x}$, $\hat{t}$. These frames, thus, have precisely the same relation to S as does S', and $\hat{S}$ equations have the same form as those for S'. Each $\hat{S}$ frame is of interest at the time $\hat{t}$ for which it is comoving with the ship. From $\hat{u}=0$ in the equations for the ship in $\hat{S}$, the coordinates at the instant of rest are

$$\hat{t}=t_{au}, \tag{9a}$$

$$\hat{x}=x_a(1-\gamma_u) \tag{9b}$$

(cf. Table I). Escort launch coordinates are $\hat{d}=\gamma_u d-\alpha_u\lambda c$ and $\hat{\lambda}=\gamma_u\lambda-\alpha_u d/c$. Note that both terminal frames are special cases of the $\hat{S}$ set, with $\hat{S}(0)=S$ and $\hat{S}(v)=S'$.

The rest frame of the ship Σ, then, comoves with an $\hat{S}(u)$ frame for all u. Except for $u=0$, the origin of Σ is offset from that of $\hat{S}$ so that the position of the ship in Σ is fixed to zero and the time to τ. The position of the escort in Σ is denoted ξ. The symbol β, without a subscript, is used for the velocity (ratio) of the escort in Σ. At any instantaneous value of τ, a ship rest event is defined by the coordinates of the ship in $\hat{S}(u)$. Define also a corollary escort event by the position coordinate of the escort in this frame at the time coordinate of the ship, that is, the escort event simultaneous in $\hat{S}$ with the rest event. The escort position ξ then is the difference in $\hat{S}$ position coordinates for the two events, and β is defined here by the escort velocity in $\hat{S}$.

The coordinates and velocity of the escort, for the corollary event of a given τ, are defined in any inertial frame, and vary widely. The escort proper time ρ, by contrast, is frame-independent, defined by the escort worldline. The definition here of $\rho(\tau)$ is the proper time of the escort at the corollary event. The solution to the acceleration problem, then, is a set of escort equations determining the escort variables $\xi(\tau)$, $\beta(\tau)$, and $\rho(\tau)$, for all τ. These variables are illustrated graphically in Fig. 1.

III. SYSTEM STATES

The escort equations are parsed according to system states defined for the two-object system. Each of the two craft, the ship and the escort, has the following three individual states:

- 0, at rest in S (parked);
- 1, accelerating (in flight); and
- 2, at rest in S' (docked).

There are then $3^2=$ nine system states ψ_{ij}, where i and j denote the individual states for the ship and the escort, respectively.

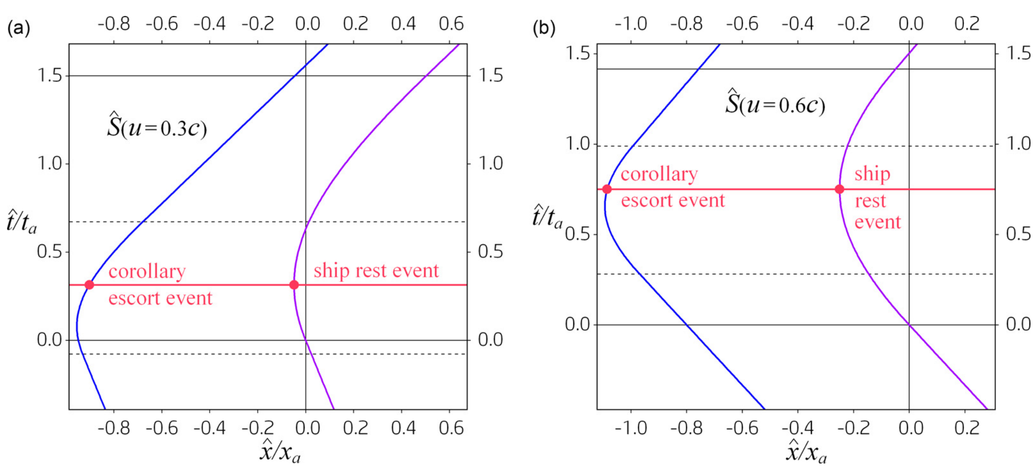

Fig. 1. Escort variables for the acceleration problem, illustrated by spacetime diagrams in $\hat{S}(u)$ for (a) $u=0.3\,c$ and (b) $u=0.6\,c$, two times $\tau(u)$ in the same spaceflight. In each diagram, the curve on the right is the worldline of the ship and the curve on the left is the worldline of the escort ($b=2a$). In the ship frame Σ, the escort position $\xi(\tau)$ is given by the difference in position coordinates $\hat{x}$ between the two events in the diagram, the escort velocity $\beta(\tau)$ is the slope of the worldline at the corollary event, and the escort proper time $\rho(\tau)$ is defined by the corollary event. The dashed lines mark escort launch and docking, and the upper solid line is ship docking. This spaceflight is discussed in Sec. V A.

The escort equations for a given system state are derived from the results in Sec. II and Lorentz transformations. Generally, for states with acceleration, the calculation includes the equations of motion of accelerating craft in the frame comoving with the ship, that is, in S, $\hat{S}$, or S' for $i = 0, 1$, or 2, respectively. Explicit derivations of the escort equations are given here for the three $j = 1$ states and for ψ_{12}, and equations for all nine states are tabulated at the end of this section.

Equation (4d) for the escort can be written as $\underline{\rho} = (\rho - \lambda)/t_b - \mu_q$, with $\mu_q = 0$ in S, $q = u$ in $\hat{S}$, and $q = v$ in S'. For state ψ_{01}, the ship frame is S, and Eq. (4c) for the escort is $t = \lambda + t_b \sinh \underline{\rho}$. Since $t = \tau$, this gives $\rho(\tau)$ directly, and $\beta(\tau)$ and $\xi(\tau)$ may be read from Eqs. (4a) and (4b), respectively.

For ψ_{11}, escort Eq. (4c) in the ship-rest frame is $\hat{t} = \hat{\lambda} + t_b(\sinh \underline{\rho} + \alpha_u)$, which, with $\hat{t} = t_{au}$ from Eq. (9a), gives $\rho[u(\tau)] = \overline{\lambda} + t_b\{\mu_u + \mathrm{arsinh}[(t_{au} - \hat{\lambda})/t_b - \alpha_u]\}$, where $u(\tau)$ is from Eq. (7a). The velocity $\beta(u)$ again follows from Eq. (4a), and $\xi(u) = \hat{d} + x_b(\cosh \underline{\rho} - \gamma_u) - x_a(1 - \gamma_u)$ from Eqs. (4b) and (9b).

For ψ_{21}, escort Eq. (4c) in S' is $t' = \lambda' + t_b(\sinh \underline{\rho} + \alpha_v)$. From Table I and Eq. (7a) with $u = v$, the ship proper time is $\tau = \tau_{av} + t' - t_{av}$, and this gives the equation for $\rho(\tau)$, with $\beta(\tau)$ and $\xi(\tau)$ specified as before.

In the case of state ψ_{12}, define

$$\phi = \frac{v - u}{1 - vu/c^2}, \tag{10}$$

the velocity of S' in $\hat{S}(u)$, so that $\beta(u) = \beta_\phi$. The time coordinate in $\hat{S}$, from Eq. (9a), and the escort position in S', from Table I, in the transformation $x' = \gamma_\phi \hat{x} - \alpha_\phi c\hat{t}$ give $\hat{x} = [d' + x_b(1 - \gamma_v)]/\gamma_\phi + \phi t_{au}$, and thus, $\xi(u)$. Then, substituting for $\hat{x}$ in $t' = \gamma_\phi \hat{t} - \alpha_\phi \hat{x}/c$ gives $t' = t_{au}/\gamma_\phi - (\beta_\phi/c)[d' + x_b(1 - \gamma_v)]$, which determines $\rho(u)$, given $\rho = \lambda + \tau_{bv} + t' - \delta'$ from Eq. (7b) and Table I.

The escort equations for the nine system states are collected in Table II. These states, except for ψ_{00}, involve accelerations directly or indirectly, and the equations reflect events, such as Eqs. (9a) and (9b), determined by Eqs. (4a)–(4d) in the coordinates of multiple inertial frames. The states in the table are arranged in triplets, in order of increasing i, and the patterns are evident. For the $j = 1$ states, each of the three escort variables has a consistent form. This follows from the derivations above, and in the table, Eqs. (6a)–(6d) are used to simplify the formulas, which enhances the similarity. With $\rho(\tau)$, there are two terms, the arsinh term plus an offset term which is, interestingly, the proper time of the escort for *its* rest event in the ship frame, $\hat{S}(0 \le u \le v)$. Also note that in the ψ_{12} formulas, which involve both u and v, the additivity of rapidities has been used.

IV. STATE SERIES AND FLIGHT SEQUENCES

The escort equations of Table II determine the escort variables $\xi(\tau)$, $\beta(\tau)$, and $\rho(\tau)$ for any system state ψ_{ij}. A particular problem is typically limited to a subset of the nine states, and each state normally applies to a range of ship proper times τ. The relations giving the system state ψ_{ij} as a function of τ come from the state series and its transition times.

The five parameters v, a, b, d, and λ on which the escort equations are based uniquely determine a series of system states. There are nine series possible, and they are fundamental, and exhaustive. To distinguish physically separate cases contained within individual series, a set of flight sequences is defined which is closely related, and supplemental, to the state series.

The sequences are divided by launch order, escort-first or ship-first, and there are three basic arrangements for the accelerations. The time intervals during which the two craft accelerate can be separate, with no time points in common; they can be inclusive, one interval contained within the other; or they can overlap, sharing some but not all points. This gives six sequence types, and each is designated with a flight index, 1–6, as defined in Fig. 2. The ship acceleration window is defined by

$$0 \le \tau < \tau_{av}, \tag{11a}$$

and the escort acceleration window is defined by

$$\tau(\lambda)|_{\min} \le \tau < \tau(\lambda + \tau_{bv})|_{\max}, \tag{11b}$$

where $\tau(\rho)$ is the inverse function of $\rho(\tau)$ from Table II, and the min/max stipulations refer to horizon cases.

The sequence is, thus, determined by the order of launch and docking events in the ship frame Σ, and this order is known from coordinates in S and S'. The order of events relative to ship launch is the same in S and Σ, and the order relative to ship docking is the same in S' and Σ. That is, for the ship, escort launch [docking] occurs before ship launch for λ [δ] < 0 and afterward for λ [δ] > 0; likewise, escort launch [docking] precedes ship docking for λ' [δ'] $< t_{av}$ and follows

Table II. Escort equations for the nine system states, ψ_{ij}, giving the escort position $\xi(\tau)$ and velocity $\beta(\tau)$ in the ship frame Σ and the escort proper time $\rho(\tau)$ for all τ, the ship proper time. Equation (7a) connects the terms in u, the velocity of the ship in S, with τ for the $i = 1$ states, and Eq. (10) defines the velocity ϕ for ψ_{12}.

ψ_{ij}	$\xi(\tau)$	$\beta(\tau)$	$\rho(\tau)$
ψ_{00}	d	0	τ
ψ_{01}	$d + x_b[f(\underline{t}) - 1]$	$\underline{t}/f(\underline{t})$	$\lambda + t_b \,\mathrm{arsinh}\, \underline{t}$, where $\underline{t} = (\tau - \lambda)/t_b$
ψ_{02}	$d - x_b(1 - 1/\gamma_v) + \beta_v c(\tau - \lambda)$	β_v	$\tau/\gamma_v + t_b(\mu_v - \beta_v) + \lambda(1 - 1/\gamma_v)$
ψ_{10}	$d/\gamma_u - x_a(1 - 1/\gamma_u)$	$-\beta_u$	$\beta_u(t_a + d/c)$
ψ_{11}	$\hat{d} + x_b[f(\hat{\underline{t}}) - \gamma_u] + x_a(\gamma_u - 1)$	$\hat{\underline{t}}/f(\hat{\underline{t}})$	$\lambda + t_b(\mu_u + \mathrm{arsinh}\, \hat{\underline{t}})$, where $\hat{\underline{t}} = (t_a\alpha_u - \hat{\lambda})/t_b - \alpha_u$
ψ_{12}	$[d' - x_b(\gamma_v - 1) + x_a(\gamma_v - \gamma_\phi)]/\gamma_\phi$	β_ϕ	$\lambda + t_b\mu_v - \lambda' - [\alpha_u(t_b - t_a) + \alpha_\phi(t_b + d'/c)]/\gamma_\phi$
ψ_{20}	$d/\gamma_v - \beta_v c[\tau + t_a(\alpha_v - \mu_v)] + x_a(\gamma_v - 1)$	$-\beta_v$	$\beta_v d/c + [\tau + t_a(\alpha_v - \mu_v)]/\gamma_v$
ψ_{21}	$d' + x_b[f(\underline{t}') - \gamma_v] + x_a(\gamma_v - 1)$	$\underline{t}'/f(\underline{t}')$	$\lambda + t_b(\mu_v + \mathrm{arsinh}\, \underline{t}')$, where $\underline{t}' = [\tau - \lambda' + t_a(\alpha_v - \mu_v)]/t_b - \alpha_v$
ψ_{22}	$d' - (x_b - x_a)(\gamma_v - 1)$	0	$\tau + \lambda - \lambda' - (t_b - t_a)(\alpha_v - \mu_v)$

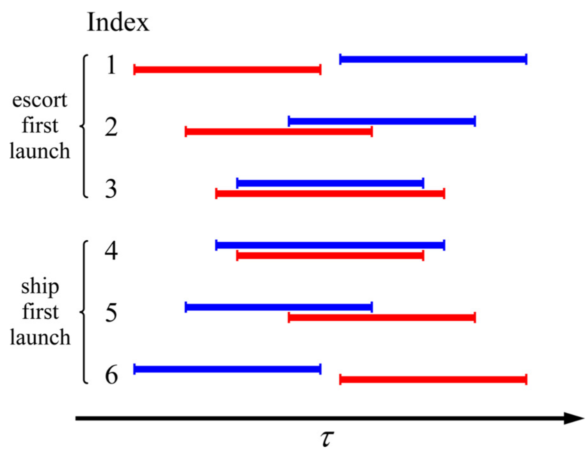

Fig. 2. Flight indexes. The acceleration periods are depicted as bars, blue (upper) for the ship and red (lower) for the escort, with time increasing to the right. Each of the two launch orders has three categories, separate (1,6), overlapped (2,5), and inclusive (3,4). The $\lambda = 0$ cases are assigned index 3 for $\delta' \ge t_{av}$ and index 4 for $\delta' < t_{av}$.

it for λ' $[\delta'] > t_{av}$. The order of the states in a sequence then can be read from the time rows of Table I.

However, because of the ship's acceleration, Σ represents a range of inertial frames from S to S', and for escorts beyond the Rindler horizon of the ship, this can lead to transitions, in Σ, in order of decreasing j. This in turn accounts for three additional state series. The escort state may change from docked to flight, or from flight to parked, or both, during the acceleration of the ship. The nine state series for the problem in essence comprise one series for each flight index and one for each of the decreasing j cases. The flight sequences then subdivide the series which apply to multiple horizon states, and serve to emphasize flight index and horizon conditions.

A. Rindler horizon

At ship launch, a Rindler horizon forms at a distance $-x_a$, behind the ship, in the direction opposite the acceleration.[1,6,12,13] The Rindler horizon is an apparent horizon, so that while events within it are unaffected by it, events beyond it cannot affect the ship during acceleration. Defining the horizon parameter, $\eta \equiv \xi(\tau = 0) + x_a$, the escort will be inside, outside, or on this horizon for η positive, negative, or zero, respectively. The state of the escort at ship launch defines a launch index $j(\tau = 0)$, and there is a state horizon parameter η_j for each j. From the ψ_{1j} equations (or the ψ_{0j} equations) in Table II,

$$\eta_0 = x_a + d, \tag{12a}$$

$$\eta_1 = \eta_0 + x_b[f(\lambda/t_b) - 1], \tag{12b}$$

$$\eta_2 = \eta_0 + x_b(\gamma_v - 1) - v\delta. \tag{12c}$$

Note that $\eta_1 = \eta_2$ for $\delta = 0$, and $\eta_1 > \eta_2$ otherwise.

For $\eta = 0$, the derivative $d\rho/d\tau$ vanishes for the duration of the acceleration, and the proper time of the escort is frozen in Σ. For $\eta < 0$, the derivative becomes negative. Because Σ comoves with multiple inertial frames, a given value of ρ can occur for more than one value of τ. This happens only for $\eta \le 0$, and it is fundamentally due to the relativity of simultaneity. Causally, the ship and the escort become disconnected in the sense that signals from the escort cannot reach the ship while it accelerates, but the ship remains visible to the escort.

An example of this behavior is an escort event d, ε with time $\varepsilon < 0$ in S for $d/c < \varepsilon/\beta_v - t_a$. This event will occur in S before $t = 0$ (ship launch) and in S' after $t' = t_{av}$ (docking). The ship is at rest in S for the event and, because of its acceleration, subsequently at rest in S' for the same event. (The event, however, is not observable to the ship in S, since $d < c\varepsilon$.) The acceleration makes it possible for a single observer to be at rest in both frames for the d, ε event, but quite apart from this, the order of events, d, ε vs. launch or docking, is opposite in the two frames.

Whereas before launch $\tau(\rho = \varepsilon) = \varepsilon$, after docking $\tau = t' + \tau_{av} - t_{av}$, which gives $\tau(\varepsilon) = \tau_{av} + \gamma_v\varepsilon - \alpha_v\eta_0/c > \tau_{av}$. During acceleration, the $\hat{S}(u)$ frame with coordinate time $\hat{t} = t_{au}$ for the d, ε event satisfies $\beta_u = \varepsilon/(t_a + d/c) < \beta_v$, giving $0 < \tau < \tau_{av}$. There are, thus, three distinct values of $\tau(\varepsilon)$, for the ship at rest in S, S', and one of the $\hat{S}(u)$ frames.

In the general case, the conditions for opposite order of occurrence in separate frames for a pair of events are $(c\Delta t)^2 < (\beta_2\Delta x)^2$ and $\beta_2\Delta x\Delta t > 0$, where Δx and Δt are the coordinate differences between events in any frame, and $c\beta_2$ is the velocity in that frame of any other frame. As described in Sec. II, the ship rest event in a given $\hat{S}(u)$ is associated with a corollary escort event. Even though, in a given $\hat{S}(u)$, the ship rest event occurs after the rest events of all slower frames, and before the events of faster frames, it can be shown from the opposite order conditions that the reverse is true for the corollary events when $\eta < 0$. That is, the ship rest event in $\hat{S}(u)$ occurs before the corollary events of slower frames, and after events of faster frames. Conversely, the corollary events occur in parallel order to the ship events when $\eta > 0$.

Figure 3 shows an example with $\eta < 0$ for two $\hat{S}(u)$ frames. In $\hat{S}(0.6c)$, Fig. 3(b), the ship rest event occurs before the corollary event of $\hat{S}(0.3c)$. Similarly, it is also clear from the escort worldlines in the two diagrams that $\rho(\tau)$ is smaller for the larger u. In Fig. 1, by comparison, $\eta > 0$, and the B and D events (not shown) both occur after ship rest in (a), while both A and C (not shown) precede ship rest in (b).

This pattern of $dt/d\tau < 0$ is reminiscent of analyses involving $\pm$Rindler coordinate wedges, in which oppositely directed accelerations in extra-horizon regions persist indefinitely.[6,7] However, the accelerations in the analysis here, which is based in Minkowski coordinates, are codirectional and transient, as well as, in many cases, separate in time.

B. Transition times

The series of system states comprising the spaceflight determine which equations in Table II are applicable, and in what order. Also important are the transition times, the proper times of the ship at which the system transitions from one state to another, that is, τ for launch and docking events. The transition times are $\tau = 0$, $\tau = \tau_{av}$, and $\tau = \tau(\rho)$ for $\rho = \lambda$ and $\rho = \lambda + \tau_{bv}$. These times are written with state index subscripts, as for example $\tau_{01,11}$ for ship launch during escort acceleration. By convention, the state indexes for all transition times are given in order of increasing i and j, regardless of the sign of $d\rho/d\tau$.

For escort launch during the ship acceleration, the $\hat{S}$ frame is identified by $\hat{\lambda} = t_{au}$, which gives

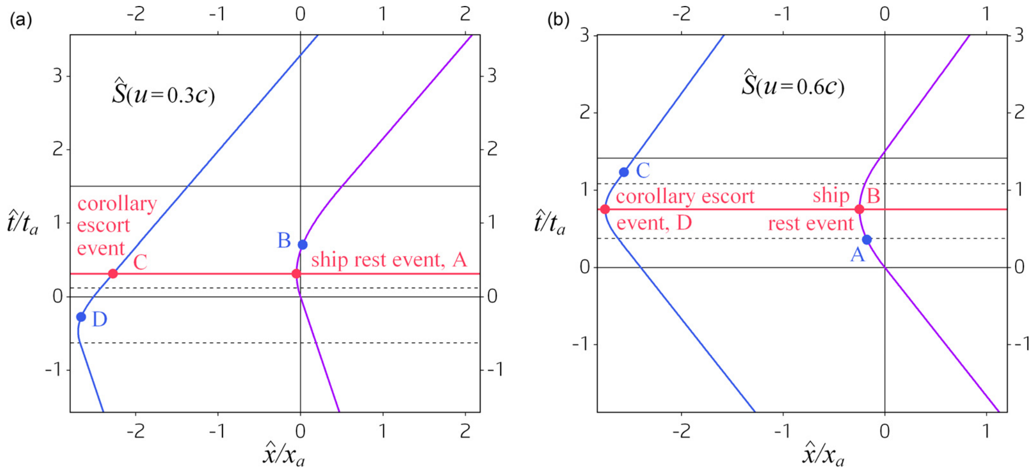

Fig. 3. Spacetime diagrams for a flight with the escort beyond the Rindler horizon of the ship. In (a) the frame is $\hat{S}(u)$ for $u = 0.3c$, and in (b), $u = 0.6c$. Events A and B are the ship rest events in the two frames, and C and D the corresponding escort events, which occur in opposite order to the ship events. In (a), the ship rest event A for that frame occurs *after* D, the escort event simultaneous with B in the faster frame (0.6), and in (b), the ship rest event B occurs *before* C, the escort event simultaneous with A in the slower frame (0.3). The solid horizontal lines mark the ship acceleration window, and the dashed lines the escort acceleration window. Further details of this spaceflight are given in Sec. V A.

$$\beta\eta_0 = c\lambda. \tag{13a}$$

If $\eta_0 \neq 0$ and the ratio is nonnegative,

$$\tau_{10,11} = t_a \operatorname{artanh}(c\lambda/\eta_0). \tag{13b}$$

When both sides of Eq. (13a) are negative, which occurs for the key combination $\eta_1 < 0$, $\lambda < 0$,

$$\tau_{av} - \tau_{10,11} \leftrightarrow \lambda' - t_{av}, \tag{13c}$$

where the double arrow is defined, *ad hoc*, to mean that the two functions have the same sign and the same zeros. That is, $\tau_{av} = \tau_{10,11}$ for $\lambda' = t_{av}$, $\tau_{10,11} < \tau_{av}$ for $\lambda' > t_{av}$ and $\tau_{10,11} > \tau_{av}$ for $\lambda' < t_{av}$.

The $\hat{S}$ time coordinate for escort docking $\hat{t} = \gamma_u\delta - \alpha_u[d + x_b(\gamma_v - 1)]/c$ leads to

$$\beta_u(\eta_2 + v\delta) = c\delta \tag{14a}$$

and again provided the ratio is nonnegative,

$$\tau_{11,12} = t_a \operatorname{artanh}[c\delta/(\eta_2 + v\delta)]. \tag{14b}$$

For the combination $\eta_2 < 0$, $\delta < 0$, both sides of Eq. (14a)—and of Eq. (13a)—are negative, and

$$\tau_{av} - \tau_{11,12} \leftrightarrow \delta' - t_{av}. \tag{14c}$$

Apart from the boundary cases $\lambda = 0$, $\delta = 0$, $\lambda' = t_{av}$, and $\delta' = t_{av}$, a system state transition changes either i or j but not both, and for simplicity, only these transitions are defined. The boundary cases are modeled as pairs of concurrent transitions. For example, the middle state in the transition pair $\psi_{00} \to \psi_{01} \to \psi_{11}$ at $0 > \lambda \cong 0$ becomes superfluous for $\lambda = 0$, but formally it remains part of the series. There are then 12 transition times, $\Delta i = 1, j = 0, 1, 2$, and $|\Delta j| = 1, i = 0, 1, 2$.

C. Flight sequence indexes

The flight sequence index consists of a flight index with a horizon index appended (see Table III). For $\eta > 0$, the horizon index is the letter h; for $\eta = 0$, the index is 0; and for $\eta < 0$, the index is the number of transhorizon states, that is, $i = 1$ states. In one instance, the same sequence index, 3.2, occurs in two series, and these cases are distinguished by a subscript giving the launch index from Eqs. (12b) and 12(c). Thus, 3.2_1 is the index for the escort-first inclusive sequence with two transhorizon states, and having $j(\tau = 0) = 1$. Note that the sequence type, e.g., sequence 3, simply identifies a sequence by flight index.

Escorts beyond the horizon also entail a second type of concurrent transition due to boundary cases. For $\eta < 0$, $d\rho/d\tau$ changes sign at $\tau = 0$ and $\tau = \tau_{av}$, and an escort transition $j \to j'$ just before one of these inflection points will quickly be succeeded by $j' \to j$. In the limit that the transition occurs at the point, the j' state will be transient, but again remains part of the series. For example, the state ψ_{12} is retained at $\tau = 0$ for $\rho(0) = \lambda + \tau_{bv}$, though immediately $\rho < \lambda + \tau_{bv}$ again and $\psi_{12} \to \psi_{11}$.

Sequences 2, 4, and 5 admit only $\eta > 0$, and the indexes are simply 2.h, 4.h, and 5.h. In sequence 2, for example, $\eta = \eta_1$, and $\eta_1 \leq 0$, which would require $\eta_0 \leq 0$ also, is disallowed because $\delta > 0$ implies $|\lambda| < t_{bv}$. That is, $\eta_0 \leq 0$ in the overlapped flight constraint $\delta' < t_{av} \to c\lambda < \beta_v(\eta_0 - x_b)$ results in $(c\lambda/\beta_v)^2 > (\eta_0 - x_b)^2$, and from Eq. (12b), $(c\lambda/\beta_v)^2 > x_b^2 + (c\lambda)^2$, which is incompatible with $|\lambda| \leq t_{bv}$.

Sequence 3 draws from both Eqs. (12c) and (12b). For sequence 1, $\eta = \eta_2$, and from Eq. (12c), $\delta' - t_{av} = [c\delta(1/\beta_v - \beta_v) - \eta_2]\alpha_v/c$. However, sequence 1 requires $\delta' < t_{av}$, and for negative η_2 of sufficient magnitude, $\delta' \to t_{av}$ and the flight index becomes 3. From Eq. (14c), $\delta' > t_{av}$ is here equivalent to $\tau_{11,12} < \tau_{av}$, and $j = 2 \to 1$ occurs at ship rest in an $\hat{S}(u)$ frame. Since $\alpha_v > \gamma_v - 1$, direct comparison of Eq. (14b) with Eq. (13b) shows that in these conditions, $\tau_{11,12} < \tau_{10,11}$, and escort launch, also, occurs at $\hat{t} = t_{au}$ in an $\hat{S}(u)$ frame if $\tau_{10,11} < \tau_{av}$, which from Eq. (13c) requires $\lambda' > t_{av}$. Another interesting combination is $\delta = 0$ and $\eta_2 = 0$, for which all values of β_u satisfy Eq. (14a), and escort docking occurs throughout ship acceleration. For the $j(\tau = 0) = 1$ launch index, the situation is similar to the $j = 2$ case, and the transition $j = 1 \to 0$ is possible during

Table III. State series and flight sequence definitions from input parameters. The state series labels are followed by the indexes, in order, for the states in that series. The transition time for each adjacent pair of states is given in Table IV. Table V summarizes the classification structure for the series. The flight index is defined in Fig. 2, and the state series are numbered by flight index, except where decreasing j transitions occur (see the text).

Flight index	λ	δ	$\lambda' - t_{av}$	$\delta' - t_{av}$	State series	Indexes ij of the series states ψ_{ij}									η launch index	Sequence index
1	< 0	≤ 0	< 0	≤ 0	1	00	01	02	12	22					$\eta_2 > 0$	1.h
															$\eta_2 = 0$	1.0
		< 0													$\eta_2 < 0$	1.1
3		≤ 0	≤ 0	> 0	1-5	00	01	02	12	11	21	22				3.2_2
			> 0		1-6	00	01	02	12	11	10	20	21	22		3.3
2		> 0	< 0	< 0	2	00	01	11	12	22					$\eta_1 > 0$	2.h
3	≤ 0			≥ 0	3	00	01	11	21	22						3.h
			≤ 0	> 0											$\eta_1 = 0$	3.0
	< 0														$\eta_1 < 0$	3.1
	≤ 0		> 0		3-6	00	01	11	10	20	21	22				3.2_1
4	≥ 0		< 0	≤ 0	4	00	10	11	12	22					$\eta_0 > 0$	4.h
5	> 0			> 0	5	00	10	11	21	22						5.h
6			≥ 0		6	00	10	20	21	22						6.h
															$\eta_0 = 0$	6.0
															$\eta_0 < 0$	6.1

the ship acceleration. Sequence 6 is much like sequence 1, though simpler.

The state series and the flight sequences are given in Table III, defined in terms of the input parameters. Six of the series have five states each and are labeled 1–6, matching the flight index for the series. The three series with decreasing j transitions are essentially combinations of the others and are given hyphenated labels. This arrangement groups two of the sequence 3 cases with sequence 1, but it preserves the order of the state indexes and groups the launch indexes symmetrically.

The series labels in the table are followed by the indexes ij of each state ψ_{ij} in the series. The transition from one state to the next occurs at the transition time identified by indexes from the two states. These times are given in Table IV, incorporating Eqs. (13b) and (14b). The sequence indexes are given in the last column of Table III, including three sequences each for series 1, 3, and 6, dividing them by horizon index, for a total of 15 sequence indexes. For clarity, an explicit classification tree for the state series is given separately in Table V. It is perhaps worth stressing that this classification applies only to the ship frame Σ. Inertial frames all have positive η sequences, and for a given flight, the index can vary with frame velocity.

D. Flight constraints

In Sec. V, examples of solutions for object arrays are given incorporating flight constraints, particularly on final conditions. Born rigidity is the prototype constraint, fixing spatial separations for point objects throughout a flight. Similarly, the final difference in position, and the net increase in age, of independent escorts relative to the ship form key metrics that are straightforward to determine, and likewise to constrain.

From the ψ_{11} equations of Table II, for $\lambda = 0$ the time variable $\hat{\underline{t}}$ vanishes for all u if

$$x_b = \eta_0. \tag{15}$$

This is the Born rigidity condition, and it results in $\xi = d$ and $\beta = 0$ for all τ. In the same vein, $x_b = \eta_0/2$ gives $\beta = \beta_u$ for all d. Both of these cases have $\rho = \tau\eta_0/x_a$. As an interesting aside, linear $\rho(\tau)$ in ψ_{11} is also possible for general λ with the constraint $(\eta_0/x_b - 1)^2 = (\lambda/t_b)^2 + 1$, which gives $\rho = \tau(1 \pm 1)t_b/t_a + \lambda - t_b \operatorname{arsinh}(\lambda/t_b)$, where the upper sign is for $\eta_0 > x_b$.

In the general case, the separation between the ship and the escort at the end of a flight sequence is

$$\xi_{[22]} = \gamma_v d - \alpha_v \lambda c - (x_b - x_a)(\gamma_v - 1), \tag{16a}$$

where $\xi_{[22]}$ denotes $\xi(\tau)$ in ψ_{22}, which is constant. The difference in elapsed proper times is

Table IV. System state transition times, where $j = 0, 1, 2$.

transition state indexes	time $\tau_{ij,i'j'}$
$0j, 1j$	0
$1j, 2j$	τ_{av}
00, 01	λ
01, 02	δ
10, 11	$t_a \operatorname{artanh}(c\lambda/\eta_0)$
11, 12	$t_a \operatorname{artanh}\{c\delta/[\eta_0 + x_b(\gamma_v - 1)]\}$
20, 21	$\tau_{av} + \lambda' - t_{av}$
21, 22	$\tau_{av} + \delta' - t_{av}$

Table V. Classification tree for state series (cf. Table III).

Parameter constraints						State series
$\delta \leq 0$			$\delta' \leq t_{av}$			1
	$\delta' > t_{av}$		$\lambda' \leq t_{av}$			1-5
			$\lambda' > t_{av}$			1-6
$\delta > 0$	$\lambda \leq 0$	$\lambda \neq 0$ or	$\lambda' \leq t_{av}$		$\delta' < t_{av}$	2
		$\delta' \geq t_{av}$			$\delta' \geq t_{av}$	3
				$\lambda' > t_{av}$		3-6
			$\lambda = 0$ and $\delta' < t_{av}$			4
	$\lambda > 0$	$\lambda' < t_{av}$		$\delta' \leq t_{av}$		
				$\delta' > t_{av}$		5
			$\lambda' \geq t_{av}$			6

$$\rho_{[22]} - \tau_{[22]} = \alpha_v d/c - (\gamma_v - 1)\lambda - (t_b - t_a)(\alpha_v - \mu_v), \tag{16b}$$

where again the subscripts denote values in ψ_{22}, and this is also constant, though of course $\rho(\tau)$ and τ are not. Equations (16a) and (16b) are from the ψ_{22} equations in Table II and apply to all sequences. They specify final conditions, but may also be used in reverse, to determine input parameters for equal, or otherwise set, docking positions or elapsed times.

For equal accelerations, the condition for equal elapsed times, from Eq. (16b), is independent of acceleration, and the final separation is $d' = \gamma_v d - \alpha_v^2 d/(\gamma_v - 1) = -d$. In fact, both Eqs. (16a) and (16b) are independent of acceleration rates both for equal accelerations and for the Born accelerations of Eq. (15).

There are three independent escort parameters in Eqs. (16a) and (16b), b, λ, and d, and only two are required to fix docking positions and elapsed times simultaneously. The launch coordinates are particularly flexible since they can take on any values, whereas the accelerations must be positive. There are limitations, however. In the important case of zero difference, $\xi_{[22]}$, $\rho_{[22]} - \tau_{[22]} = 0$, substitution of Eqs. (16a) and (16b) into Eqs. (12a)–(12c) shows that $\eta > 0$ is required, and the escorts must remain within the Rindler horizon. These constraints are illustrated in Sec. V B.

V. RESULTS AND DISCUSSION

The solution to the acceleration problem then is determined. Given a set of input parameters, Table V specifies the state series, with the states of each series listed in Table III, which also gives the sequence index. An accompanying list of transition times for the series, one time for each pair of successive states, is given by Table IV. The state of the system, then, for any particular value of τ is identified by the transition times, and the escort variables $\xi(\tau)$, $\beta(\tau)$, and $\rho(\tau)$ for that state are calculated from Table II. The start time for the problem is the smaller of λ and zero, and the end time is the larger of τ_{av} and $\tau_{21,22}$. For additional escorts, the procedure is the same. Each escort has its own set of parameters, b, d, and λ, with the final velocity v and the ship acceleration a common to all. Solutions for alternate choices of host in turn require only offsets to the launch coordinates, as illustrated at the end of Sec. V B.

Section V A surveys the nine state series for the two-object problem, giving solutions for representative examples, and Sec. V B demonstrates practical application of the general solution for object arrays. The array problems include acceleration both of integral rods and of independent objects, and illustrate constraints from Sec. IV D.

In all cases, it is the position $\xi(\tau)$, velocity $\beta(\tau)$, and proper time $\rho(\tau)$ of the companion object(s) in the noninertial rest frame of the host, Σ, that are central, and the host proper time τ is the independent variable. The results of the calculations are plotted with τ on the horizontal axis, and ξ, β, and ρ on the vertical axes. For convenience and generality, the graphs are presented in a dimensionless format.

The acceleration problem can be nondimensionalized by normalization, dividing Eq. (4b) by x_a, Eq. (4c) by t_a, and Eq. (4a) by c, in the equations for both craft and the forms for all frames (S, $\hat{S}$, and S'). The input parameters are reduced in number to β_v, a/b, d/x_a, and λ/t_a. The normalized solution then gives ξ/x_a, ρ/t_a, and β as functions of τ/t_a. The dimensionless version of Table II ($\xi \to \xi/x_a$, etc.) is unchanged in appearance except that a and c are absent.

The normalized solution is obtained here from the unnormalized equations by choosing units with $|c| = 1$ and setting $|a| = 1$. The normalized solution may then be applied to arbitrary accelerations a in any system of units. In the graphs, the dimensionless variables are denoted with colored symbols, $\xi\,(\text{blue}) = \xi/x_a$, $\beta\,(\text{green})$, $\rho\,(\text{red}) = \rho/t_a$, and $\tau\,(\text{brown}) = \tau/t_a$, blue, green, red, and brown, and the plotted curves are likewise color-coded. In the text, quantities are dimensioned.

For the spacecraft, the values $t_a = 1$ (Julian) year (y) and $x_a = 1$ light-year (ly) lead to the unit of acceleration, 1 ly/y/y, which is defined as a standard value

$$a_G = 9.500\,\mathrm{m\,s^{-2}}, \tag{17a}$$

approximately equal to $1\,\mathrm{g} = 9.807\,\mathrm{m\,s^{-2}}$. A second, far larger, acceleration

$$a_H = 9.461 \times 10^{15}\, a_G, \tag{17b}$$

is defined for which $x_a = 1$ m and $t_a = 3.336$ ns. A standard velocity of $v_0 = \sqrt{3}/2\,c = 2.596 \times 10^8\,\mathrm{m\,s^{-1}}$ is used for all the solutions ($\gamma_{v_0} = 2$). Although the inertial frames S, S', and $\hat{S}(u)$ are discussed at various points in this section, the graphs are confined to the variables in the noninertial frame Σ.

A. State series

In this subsection, we survey the spectrum of acceleration cases for two objects, the ship and its escort. Figures 4–6 give examples of the nine state series, three series per graph. The cases in a single graph are chosen to have nonintersecting $\xi(\tau)$ curves for clarity. The $\rho(\tau)$ plots start together, increasing diagonally, and the $\beta(\tau)$ curves, referred to the right axis, begin and end at zero. The shaded area is the ship acceleration region, flanked by the dark vertical lines marking ship launch and docking. The other vertical

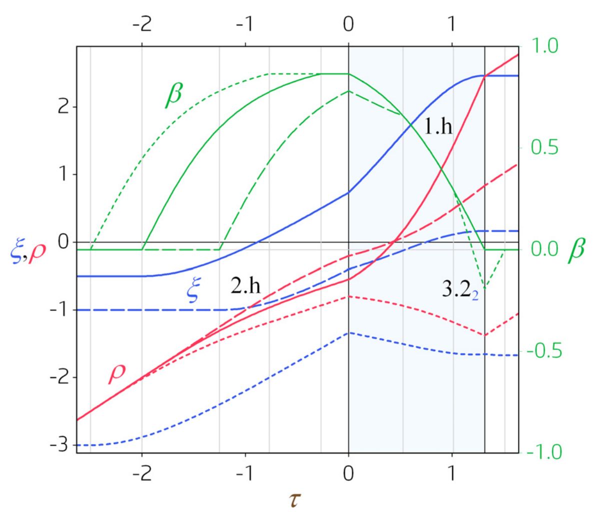

Fig. 4. State series 1, 1-5, and 2 examples with $b = a$. Sequence 1.h, solid lines; 3.2_2, short dashes; 2.h, long dashes. d is always the initial value of ξ. $\lambda < 0$ can be read from the τ axis (launch transitions).

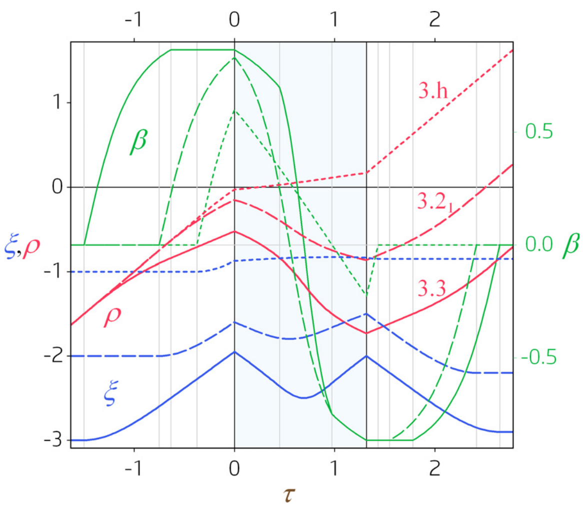

Fig. 5. State series 3, 3-6, and 1-6 examples with $b = 2a$. Sequence 3.h, short dashes; 3.2_1, long dashes; 3.3, solid lines.

lines are escort transition times. Also, small time segments are included at either end, before the first launch and after the last docking. For $a = a_G$, these graphs may be read as having units y (τ, ρ) and ly (ξ).

In Fig. 4, the escort launches first. For series 1 (seq. 1.h) and series 2 (seq. 2.h), the flights are, respectively, separate and overlapped in the ship frame Σ, and also in the terminal frames, S and S' (not shown). For the transhorizon case, the spaceflight in S is series 1 and in S' it is series 5, while in Σ, it is series 1-5, a hybrid comprised of the first four states of series 1 and the last three of series 5 (Table III). The escort docks at $\tau = -0.77\, t_a$, but if the ship launches on schedule at $\tau = 0$, the escort docking will not be observed by the ship before launch and will be unobservable during acceleration. At $\tau = 1.02\, t_a$, the ship is momentarily at rest in $\hat{S}(u = 0.77\, c)$, and in this frame the escort is docking at that instant. This is the second of the two escort transition times shown in the ship window of the graph. The ship then docks at $\tau = \tau_{av}$, and escort docking in S' occurs afterward (at $\tau = 1.51\, t_a$), in accordance with the series 5 order.

Sequence 1.h in Fig. 4 shows another interesting feature of acceleration. Just before ship launch the escort is at rest in S', with constant velocity v away from the ship, and ξ is increasing linearly. When the ship launches, the velocity of the escort begins to decrease as the ship accelerates toward it, but the distance between the two craft, rather than slowing its rate of increase, actually does the opposite. That is, $d\xi/d\tau$ increases.

The escorts in Fig. 5, as in Fig. 4, have negative launch times, and in this group all three flights are inclusive. Series 3 (seq. 3.h) is straightforward, and interesting in that the escort docks before the ship in S and launches after it in S', so that those sequences are 2.h and 5.h. It is from this series 3 case that the two $\hat{S}(u)$ diagrams in Fig. 1 are taken. The other two flights in Fig. 5 have $\eta < 0$, and both have decreasing j transitions, series 3-6 (seq. 3.2_1) with one and series 1-6 (seq. 3.3) with two. Due to the combination of launch coordinates, two of these three transitions actually occur at the same time, at $\tau_{10,11} = 0.97\, t_a$. However, the $j = 0 \to 1$ transitions outside the ship window, at $\tau_{00,01}$ and $\tau_{20,21}$, are distinct for the two flights. Sequence 3.3, series 1–6, is unique in that it includes all nine states. It is essentially a merger of series 1 and 6, and these are the series for the flight in S and S', which, thus, have separate acceleration windows in opposite order. The $\hat{S}(u)$ diagrams of Fig. 2 are taken from this flight. Note that all of the $\eta < 0$ cases in Figs. 4 and 5 illustrate the general result, described in Sec. IV, that each transhorizon transition is echoed both before and after the ship acceleration window, with the value of ρ (either λ or $\lambda + \tau_{bv}$) common to all three transitions.

The series in Fig. 6 are ship-first launch order. The separate flight case, sequence 6.0, is chosen to have $\eta = 0$. The 4.h sequence is notable for the brevity of the escort acceleration ($\tau = 0.26$–$0.44\, t_a$). This is due in part to the higher acceleration rate of the escort and in part to its forward placement. Large d tends to make the escort transition times in the ship window similar (Table IV).

As an example of units application, when the 4.h escort in Fig. 6 docks at $\tau = 0.44\, t_a$, the escort variables have values $\xi = 3.095\, x_a$, $\rho = 1.658\, t_a$, and $\beta = 0.704$. In SI units for $a = g/2$, $t_a = 6.114 \times 10^7$ s and $x_a = 1.833 \times 10^{16}$ m, so that the distance of the escort to the ship is $\xi = 5.673 \times 10^{16}$ m and the escort clock reads $\rho = 1.014 \times 10^8$ s.

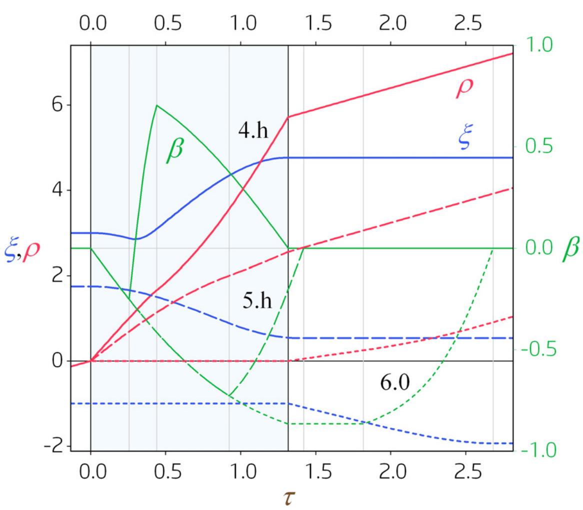

Fig. 6. State series 4, 5, and 6 examples with $b = 2a$. Sequence 4.h, solid lines, $\lambda = t_a$; 5.h, long dashes, $\lambda = 2t_a$; 6.0, and short dashes, $\lambda = t_a/4$.

B. Object arrays

The spaceflight of the ship and its escort is easily extended to multiple escorts, and the kinematics apply on any scale. The three escort flights in Fig. 4, for example, are presented separately, but the three *could* accompany the same ship on a single mission. Moreover, the calculations of the graph apply to arbitrary time (or distance) scales. If $a = a_H$, for example, the companion objects have initial positions at one-half meter, 1 m, and 3 m behind the host object and begin their accelerations, respectively, at $\tau = 6.67$, 4.17, and 8.34 ns before the host.

This subsection presents examples of object arrays. Solutions for the accelerations of elastic and rigid rods, in which the objects represent points along the integral structure of the rod, are treated in detail (Figs. 7 and 8). As discussed in Sec. IV D, the acceleration constraint for a rigid rod, Eq. (15), has analogs in the constraint of arrival positions and elapsed proper times for independent objects, given by Eqs. (16a) and (16b). Based on these equations, an example is given of acceleration rates used to prescribe equal aging (Fig. 9), followed by several examples constraining

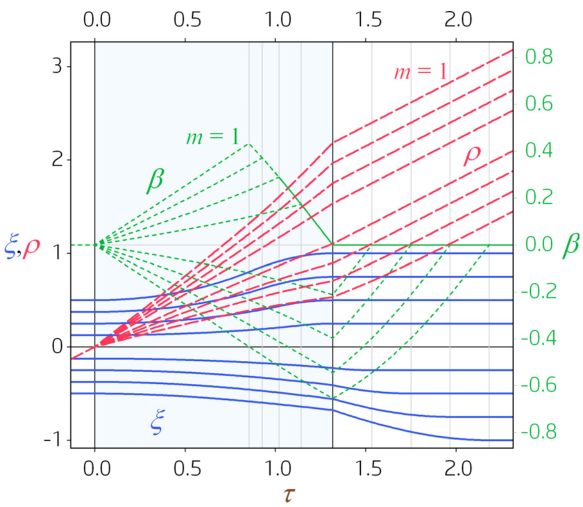

Fig. 7. Evenly spaced point objects with equal start times and accelerations, a train of spacecraft (large x_a), or an elastic rod (small x_a).

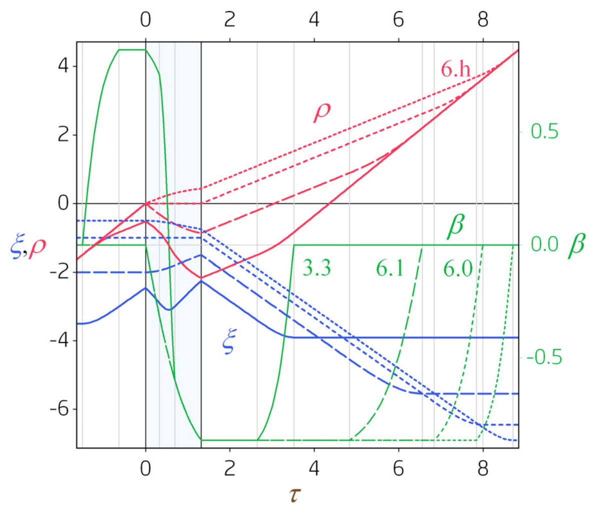

Fig. 10. Launch times set to equalize elapsed proper times for objects spanning the Rindler horizon, sequences 6.h, 6.0, 6.1, and 3.3. $b_m = 2$, 1.5, 1, and $2\,a$, $\lambda_m = 3.7$, 2.8, 0.89, and $-1.5\,t_a$.

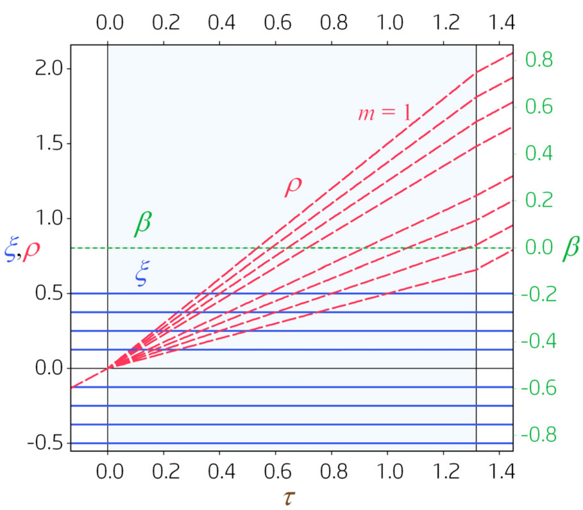

Fig. 8. Acceleration of a rigid rod (or other array). Case of Fig. 7 but with accelerations set by the Born rigidity condition, Eq. (15).

proper times and final positions by choice of launch coordinates (Figs. 10–12).

The index m is used for an array of objects. The acceleration and launch coordinates are b_m, d_m, and λ_m, and the objects are indexed from front to back, in order of decreasing d_m. The object variables are ξ_m, β_m, and ρ_m. The host is denoted by m^*. Thus, $a = b_{m^*}$, $d_{m^*} = \lambda_{m^*} = \xi_{m^*} = \beta_{m^*} = 0$, and $\tau = \rho_{m^*}$ is the independent variable of the problem.

Figure 7 shows eight companion objects with simultaneous launches, equal accelerations and evenly spaced launch points d_m in either direction from the host object. The sequences are 4.h for the leading companions and 3.h for the trailing companions. The object indexes are $m = 1$–9 with $m^* = 5$.

For $a = a_G$, $d_1 - d_9$ is 1 ly, and Fig. 7 is appropriate to a spacecraft train. The trip time aboard the ship is $\tau_{av} = 1.317\,\mathrm{y}$, while the escort trip times range from $\tau = 0.8534\,\mathrm{y}$ for the lead escort to $2.183\,\mathrm{y}$ for the trailing escort. However, although the lead escorts arrive early, in

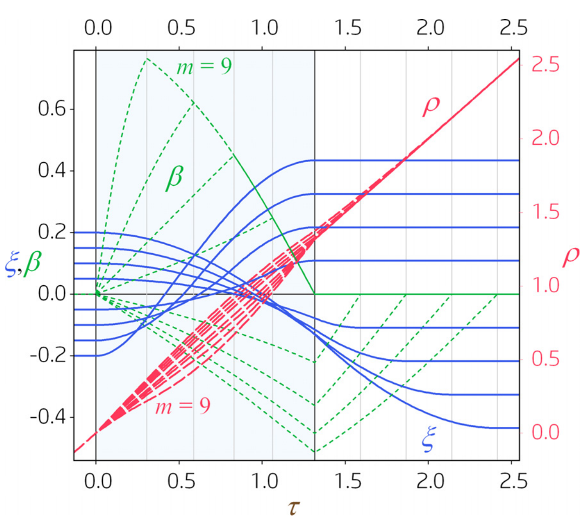

Fig. 9. Accelerations b_m set to equalize elapsed proper times for all objects. Even spacing, $\lambda_m = 0$, $b_m = 0.55$, 0.62, 0.71, 0.83, 1.26, 1.72, 2.67, and $6.04\,a$.

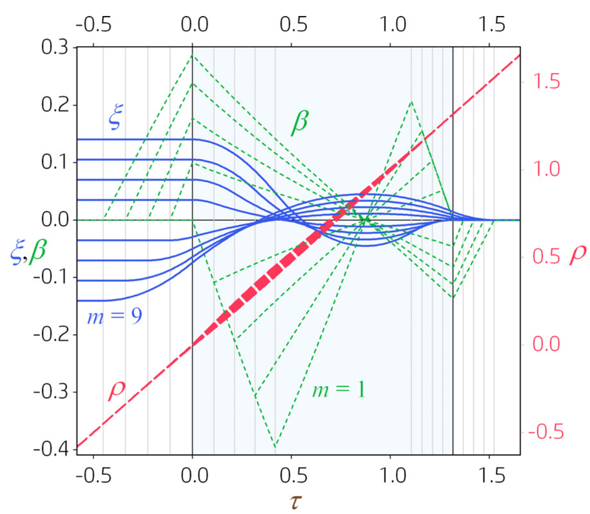

Fig. 11. Companion accelerations from Fig. 8 with launch coordinates chosen such that the docking positions and elapsed proper times of the companions match those of the host ($m^* = 5$). The object index of companion 8 is $m = 9$.

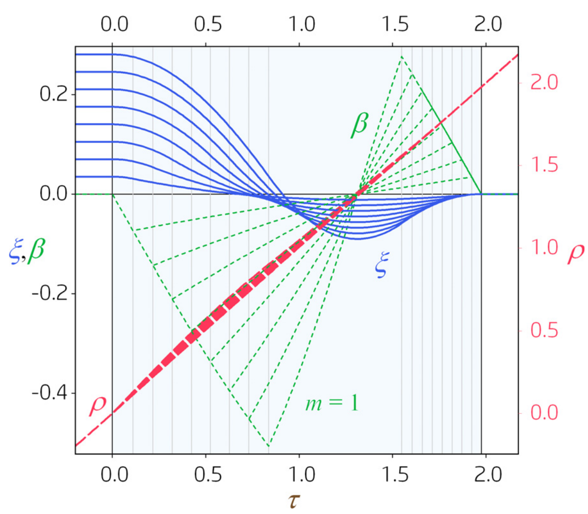

Fig. 12. Case of Fig. 11 in the rest frame of companion 8 there ($m=9$). Companion 8 here is the former companion 7, and companion 5 here is the former host. Here $m^*=9$.

the end they age more. The onboard trip time for each escort is of course the same as that for the ship, $\tau_{b_m v}=\tau_{av}$, but the leading escorts age at rest in S' waiting for the trailing escorts to arrive. The result is that, for $\tau \geq 2.183$ y, when $d\rho/d\tau=1$ again for all escorts, the lead escort has aged 3.049 y and the last escort 1.317 y. The difference is, by Eq. (16b), $\alpha_v(d_1-d_9)/c=1.732$ y. The acceleration distance in S or S' (not shown) is the same for all craft, $|\pm x_a(\gamma_v-1)|=x_a=1$ ly, and the acceleration time is $t_{av}=1.732$ y, which, in this case, is the same as the age differential since $d_1-d_9=x_a$.

For $a=a_H$, d_1-d_9 is 1 m, and the Fig. 7 data become a solution for evenly spaced points on an accelerating elastic rod. The elapsed proper time for the midpoint of the rod (the host point) is 4.393 ns, and in the frame of that point, the trip times for the leading and trailing tips of the rod are 2.847 and 7.282 ns, respectively. When the last of the rod comes to rest in S', it has aged 4.393 ns, as compared to 10.17 ns for the leading edge. The acceleration distance and time in the terminal inertial frames are, respectively $x_a=1$ m and $t_{av}=5.778$ ns. Again, this is true for all points, though in S' the different parts of the rod launch (and dock) at different times. Also note that, whatever the scale, the separation of the objects increases in S' by a factor of $\gamma_v=2$, from Eq. (16a).

For a rigid rod, if the point objects are to maintain their separations, acceleration must conform to Eq. (15), applicable within the Rindler horizon ($\eta_0>0$). Figure 8 gives results for the launch coordinates of Fig. 7 ($\eta_0 \geq x_a/2$) with the Born accelerations $b_m=a/(1+d_m/x_a)$. All points of the rigid rod are stationary in Σ and come to rest in S' at the same time, but the elapsed proper time is again greater for the leading edge. If the acceleration of the midpoint is $a=a_H$, the leading edge ages 6.589 ns and the trailing edge 2.196 ns, for a difference of 4.393 ns. For the case $a=a_G$, $\tau_{av}=1.317$ y would be the age difference between leading and trailing escorts. In S or S', the acceleration distance and time for the midpoint, or ship, are the same as for the elastic case.

As described earlier, the final spacing and differential aging for $b_m=a$ and for Eq. (15) do not depend on the rate of acceleration, but only on velocity. Thus, both the elastic and rigid rod problems have the same $\xi_{[22]}$ and $\rho_{[22]}-\tau_{[22]}$ results from Eqs. (16a) and (16b) for accelerations more tenable than a_H. With $a=10^7 a_G$, for example, a railgun value,[14] the acceleration period in the launch frame is 5.5 s, albeit with a travel distance of $\sim 10^6$ km.

For any configuration of array objects, once the accelerations have been completed, the differences in position and proper time between the companions and the host are given by Eqs. (16a) and (16b). Of particular interest are zero-difference constraints, in which final positions or times are the same for the companions and the host.

For example, from Eq. (16b) with $\lambda=0$, the accelerations required to match the elapsed proper times of companions to that of the host are $x_{b_m}=x_a+d_m/(1-\mu_v/\alpha_v)$. This imposes a lower limit on the launch positions, requiring $\eta_0>x_a\mu_v/\alpha_v$, where $\mu_v/\alpha_v \cong 0.76$ for $v=v_0$. For even spacing about a central host as in Fig. 7, the minimum d_m is accordingly set to $-0.2\,x_a$, and Fig. 9 gives the resulting trajectories. The companions reverse their positions, fore and aft, as with the equal acceleration case described in Sec. IV D ($d'=-d$), while their proper times never diverge very far from the host time. Note that the accelerations range over an order of magnitude.

Launch coordinates may also be used to impose constraints from Eqs. (16a) and (16b), and generally provide greater latitude than accelerations. From Sec. IV D, zero-difference requires companions inside the Rindler horizon, but if the host itself is excluded from the constraint, it is possible to arrange, for example, equal aging among companions on opposite sides of the horizon. This is illustrated in Fig. 10. The sequences are 6.h, 6.0, 6.1, and 3.3, with $m^*=1$. Parameters b_5, d_5, λ_5 are set for sequence 3.3, and for $1<m<5$, the b_m are set to a mix of values, the d_m for η_0, and the λ_m to match the $m=5$ value of $\rho_{[22]}-\tau_{[22]}$ from Eq. (16b). The forward companion (6.h) launches last, and also docks last, at $\rho_2=4.355\,t_a$. This value $\rho_2=\rho_m$ is then the proper time of all companions at that host time, which is $\tau=2\rho_m$.

In Fig. 11, launch coordinates are chosen to equalize both elapsed times and final positions for all objects, resulting in $\eta>0$ for all companions. The Born accelerations b_m of Fig. 8 are used, as an example, with λ_m, d_m determined by Eqs. (16a) and (16b) to achieve $d'_m+x_{b_m}(1-\gamma_v)=x_a(1-\gamma_v)$ and $\rho_m(\tau>\tau_9)=\tau$ for all m, where $\tau_9=1.525\,t_a$ is the last docking time. The onboard clocks of all objects remain very nearly synchronized for the duration of the flight. The trailing companions launch early and overtake the host, and the lead companions launch late and are overtaken, thus reversing the spatial order of companions before they converge on the host at the end.

Given a solution in the rest frame of object m^*, the corresponding solution in the rest frame of object $m=n$ is obtained by shifting the launch coordinates. The new parameters, denoted with a ~, are given by

$$\tilde{b}_m=b_m, \tag{18a}$$

$$\tilde{d}_m=d_m-d_n, \tag{18b}$$

$$\tilde{\lambda}_m=\lambda_m-\lambda_n \tag{18c}$$

for all m, and

$$\tilde{m}^*=n. \tag{18d}$$

As an example, Fig. 12 gives the case of Fig. 11 in the rest frame of the trailing companion, $n=9$ in Eq. (18).

This object was actually the lead companion in Fig. 8, with the smallest acceleration, $b_1 = 2a/3$, but in Fig. 11, it has the minimum d, and it becomes the host in Fig. 12. If $a = a_G$ in Figs. 7, 8, and 11, then $a = 2a_G/3$ in Fig. 12. The companions of Fig. 12 all have launch positions in front of the host, and their trajectories follow the pattern of the leading companions in Fig. 11.

One further point warrants mention. In applying the results for point objects to extended bodies like spacecraft, having finite proper length ℓ, we specifically require $\ell \ll x_a$ and assume that ℓ is constant, with the body acceleration satisfying the Born rigidity condition. The variation in force acting along the body is in this case a tiny fraction of the propulsive force. That is, taking a and b in Eq. (15) to be the accelerations at either end of the body, $d \to \ell \ll x_a$ implies $\Delta a = a - b \ll a$. For example, if $a = 1\,\mathrm{g}$ and $\ell = 1\,\mathrm{km}$, $\Delta a/a \cong 10^{-13}$. Note though that Δa, however small, is necessary for fixed proper length and uniform acceleration has $\ell \to \gamma_v \ell$ at rest in S' (cf. Figs. 7 and 8).

C. Concluding remarks

Formulas for the position, velocity, and proper time of the objects in an accelerating array for the noninertial rest frame of an arbitrary host object in the array have been derived and illustrated. The general solution to this problem is based on nine series of two-object states, with each state, of which there are also nine, defined by acceleration statuses. In a given problem, one of the nine series applies to each companion object, and the object's motion in each state is determined by a simple set of equations. The resulting behavior of the companions in the host frame is dominated by the fluidity of event coordinates in inertial frames of differing velocity, and the most striking examples are of companions beyond the Rindler horizon of the host, for which time runs backward in the host frame, in the sense that the host remotely revisits successively earlier companion events as the host progresses forward in time.

Among the important examples of accelerated object arrays are accelerations of rigid and elastic rods. With inflexible spatial order, the elapsed proper time, or aging, is greater for leading objects than for trailing objects. For independent objects, by analogy with the differential acceleration required to support rigidity, given by the Born condition, differential acceleration or—better—variable launch coordinates may be used to ensure equal aging, or common destinations, or both.

All array solutions are built on the pair problem of Secs. II–IV, and the two-object examples given above to illustrate the state series, thus, underpin the whole of this section. We close with a thought experiment in which a spaceflight of the ship and its escort are visualized from photos made by independent observers during the flight. An observer is stationed in selected instantaneous rest frames at the rest position of the ship (but at a distance along the $\hat{y}$ axis) to take a snapshot of the ship at the moment of rest. A second observer in each frame is located at the ($\hat{x}$) position the escort will occupy at that moment, to take a snapshot of it. The photos record the time of the clocks aboard the craft, the firing of their engines, and for the escort, the length contraction due to its speed. After the flight, the snapshots from all observers are compiled to make a video in which the spacing between the images of the two craft is proportional to, but much smaller than, the actual distance between the spaceships, and the video frame rate can likewise be adjusted. In this way, a realistic sense of the flight from a bystander's viewpoint is conveyed with the times and distances scaled to human terms. Animations simulating such a scheme for the examples of Sec. V A have been constructed.[15]

ACKNOWLEDGMENTS

The author wishes to thank the many upon whose work this paper is built, including but not limited to authors explicitly cited in the References section, and all those who have contributed during the review process. Also, special thanks are due to the National Aeronautics and Space Administration for decades of support and opportunity.

AUTHOR DECLARATIONS

Conflict of Interest

The author has no conflicts to disclose.

[a]ORCID: 0009-0004-9975-2970.

[1]M. P. Hobson, G. P. Efstathiou, and A. N. Lasenby, *General Relativity: An Introduction for Physicists* (Cambridge U. P., Cambridge, 2006), pp. 21, 2, 5, 19, 20, 125, and 126.

[2]See https://en.wikipedia.org/wiki/Acceleration_(special_relativity) for "Acceleration (special relativity)" (accessed January 10, 2023).

[3]Hrvoje Nikolic, "Relativistic contraction of an accelerated rod," Am. J. Phys. **67**, 1007–1012 (1999).

[4]Alon Drory, "Comoving frames and the Lorentz-Fitzgerald contraction," Am. J. Phys. **87**(1), 5–9 (2019).

[5]Ashok K. Singal, "Lorentz contraction during acceleration from one inertial frame to another," Am. J. Phys. **88**(7), 551–557 (2020).

[6]W. Rindler, "Kruskal space and the uniformly accelerated frame," Am. J. Phys. **34**(12), 1174–1178 (1966).

[7]P. M. Alsing, I. Fuentes-Schuller, R. B. Mann, and T. E. Tessier, "Entanglement of Dirac fields in noninertial frames," Phys. Rev. A **74**(3), 032326 (2006).

[8]Filip Kiałka, Alexander R. H. Smith, Mehdi Ahmadi, and Andrzej Dragan, "Massive Unruh particles cannot be directly observed," Phys. Rev. D **97**(6), 065010 (2018).

[9]Jean-Luc Thiffeault, M. Purcell, and R. Correll, see https://www.researchgate.net/publication/2273688_What_a_Rindler_Observer_Sees_in_a_Minkowski_Vacuum for "What a Rindler Observer Sees in a Minkowski Vacuum" (1998).

[10]See https://en.wikipedia.org/wiki/Four-acceleration for "Four-Acceleration" (accessed December 15, 2022).

[11]J. Russo and P. Townsend, "Relativistic kinematics and stationary motions," J. Phys. A **42**, 445402 (2009).

[12]Kip S. Thorne and Roger D. Blandford, *Relativity and Cosmology: Volume 5 of Modern Classical Physics* (Princeton U. P., Princeton, NJ, 2021), pp. 1186–1188.

[13]Greg Egan, see https://www.gregegan.net/SCIENCE/Rindler/RindlerHorizon.html for "The Rindler Horizon," (accessed July 5, 2022).

[14]See https://www.sciencedirect.com/topics/physics-and-astronomy/electromagnetic-acceleration for "Electromagnetic Acceleration" (accessed September 10, 2022).

[15]C. Dobson, see <eyefarer.net/physics/relativity/arrayacceleration/stateseries.html> for "Relativistic Acceleration Animations" (accessed July 2, 2023).